Assessment of Membrane-Bound Mammal Mitochondrial Adenine Nucleotide Translocase Topography by Experimental Antibodies†

Belén Notario, Carlos Manchado, Mónica Zamora, Teresa Mampel, and Octavi Viñas*

Departament de Bioquímica i Biologia Molecular, Facultat de Biologia, Universitat de Barcelona Diagonal 645, E-08028 Barcelona, Spain

Received August 13, 2002; Revised Manuscript Received November 7, 2002

ABSTRACT: To gain insight into the immunogenicity of mitochondrial adenine nucleotide translocase (ANT), we raised antibodies against purified bovine heart ANT by induction of ascitic fluid in male Balb/c mice. We identified the antigenic determinants detected by these antibodies by (1) immunodetection of GST−ANT fusion proteins and selected partial constructs of ANT, (2) immunodetection of chemically synthesized overlapping peptides on solid support, and (3) back-titration ELISA. Results revealed a short epitope spreading of the antibodies, resulting in a small number of antigenic determinants. Thus, each antibody detects one or two major epitopes located in the putative hydrophilic loops M2 and M3. No evidence for the antigenicity of the first 133 amino acids of ANT was obtained. These well-characterized antibodies were used to study the topography of the membrane-bound ANT by back-titration ELISA with mitochondrial membranes. We demonstrated that amino acids 145−150 and 230−237 are fully accessible to the antibodies in native ANT, whereas regions 133−140 and 244−251 are not. Furthermore, we used mitochondria devoid of the outer membrane (mitoplasts) and inside-out submitochondrial particles (SMP) to establish the matrix or cytosolic orientation of loops M2 and M3. The results clearly show that these loops have a matrix orientation and thus support the six transmembrane segment model of ANT topography in the inner mitochondrial membrane.

Adenine nucleotide translocase (ANT)[1] is an integral membrane protein localized in the inner mitochondrial membrane, where it catalyzes the exchange of adenine nucleotides, importing cytosolic ADP to the mitochondria for oxidative phosphorylation and exporting ATP to the cytosol (*1*). The topography of ANT in the inner mitochondrial membrane has been probed with specific antibodies against the N-terminal and C-terminal end peptides (*2*), by limited enzymatic proteolysis (*3*), by binding of azido-derived substrates (*4*) and inhibitors (*5*), and by chemical modification of specific amino acids with SH reagents (*6*, *7*) or pyridoxal phosphate (*8*) among others. The results obtained with all of these methods have been controversial. A model of six transmembrane domains, with the N-terminal and the C-terminal ends facing the cytosol and the three hydrophilic loops (M1−M3) facing the matrix, has been widely reported, yet another model has also been proposed (*3*). This alternative model states that ANT consists of five transmembrane domains with the N-terminal end facing the cytosol and the C-terminal end facing the matrix. Furthermore, loop M1 would be exposed to the matrix and loops M2 and M3 would be in the cytosolic compartment. Although the recent preparation of functional covalent dimers linked by the N-terminal and the C-terminal ends has given support for the six transmembrane segment model for the yeast ANT (*9*, *10*), direct assessment of the membrane orientation of loops M2 and M3, which could help us to decide between models, has not been reported.

ANT is a target for autoantibodies in idiopathic dilated cardiomyopathy (IDCM), and the inhibitory effect of these antibodies on ANT activity may be involved in the progression of the disease (*11*). Recently, we have demonstrated that the autoantibodies against ANT in IDCM are directed to the C-terminal half of the protein, especially to short sequences predicted to belong to the hydrophilic loops M2 and M3 of the mature protein (*12*). The absence of significant antigenic determinants in the N-terminal half of ANT was unexpected, since the prediction of the antigenicity of ANT showed several antigenic determinants in this region (*13*). Hence, whether the antigenic determinants defined in human IDCM patients reflect their higher immunogenicity or are a specific response of the disease remains to be established.

We prepared mouse antibodies against purified ANT from bovine heart mitochondria. We then identified the amino acid sequences recognized by these antibodies using immunoblots with recombinant ANT proteins, precise partial constructs, and synthetic peptides. Finally, we used the antibodies to determine the orientation of specific regions of loops M2 and M3 in back-titration ELISA with mitoplasts and inside-out submitochondrial particles (SMP). We present evidence that (i) loops M2 and M3 contain the most immunogenic regions of ANT, (ii) regions 145−150 and 230−237 are accessible to the antibodies in the native ANT, and (iii) the

† This work was supported in part by a grant (PM1999-0171) from the Ministerio de Ciencia y Tecnología (Spain) and by a grant (2001-SGR-00117) from the Generalitat de Catalunya (Spain).

* Corresponding author. E-mail: ovinas@ub.edu.

[1] Abbreviations: ANT, adenine nucleotide translocase; EMA, eosin 5-maleimide; GST, glutathione *S*-transferase; IDCM, idiopathic dilated cardiomyopathy; NEM, *N*-ethylmaleimide; PAGE, polyacrylamide gel electrophoresis; PBS, phosphate-buffered saline; PMSF, phenylmethanesulfonyl fluoride; PVDF, polyvinylidene fluoride; SDS, sodium dodecyl sulfate; SMP, submitochondrial particles.

10.1021/bi020528b CCC: $25.00
Published on Web 12/31/2002

matrix orientation of loops M2 and M3 supports the six transmembrane domain model of ANT conformation in the inner mitochondrial membrane.

EXPERIMENTAL PROCEDURES

Purification of Bovine Heart Mitochondria, Mitoplasts, and SMP. Bovine heart mitochondria were obtained by differential centrifugation as described elsewhere (*14*). Mitoplasts, i.e., mitochondria devoid of outer mitochondrial membranes, were obtained by freeze−thaw cycles of purified mitochondria as described (*2*). Inside-out submitochondrial particles (SMP) were obtained by sonication of mitoplasts as reported elsewhere (*15*, *16*). The inside-out membrane orientation of the SMP was checked by back-titration ELISA using a monoclonal antibody against subunit IV of the cytochrome oxidase (20E8-C12; Molecular Probes). This antibody reacts with an epitope of the protein which is located at the intermembrane space of mitochondria (*17*). The protein concentration was measured using the Pierce protein assay reagent (Pierce Chemical Co). The intactness of mitochondria, mitoplasts, and SMP was confirmed by electronic transmission microscopy (SCT; University of Barcelona) and by the ability of these preparations to oxidize exogenous NADH, measured using a UV−visible recording spectrophotometer (Shimadzu UV-160A). Fragments of mitochondrial membranes were obtained by treating purified mitoplasts with a hypotonic solution (5 mM Tris-HCl, 8 mM PBS pH 7.4), followed by three freeze−thaw cycles and sonication.

Purification of ANT from Bovine Heart Mitochondria. Mitochondrial membrane proteins were solubilized with 100 mmol/L NaCl, 1 mmol/L PMSF, 2% Triton X-100, and 20 mmol/L Hepes, pH 7.4, and adsorbed to hydroxyapatite, which had been equilibrated with 50 mmol/L NaCl, 1 mmol/L PMSF, 0.5% Triton X-100, and 20 mmol/L Hepes, pH 7.4, in a batch-method format (50 mg of hydroxyapatite/mg of mitochondrial protein). The nonadsorbed material was highly enriched in ANT, which was further purified using ChromaPhor (Promega) following the manufacturer's instructions in a low (0.035%) SDS−12% PAGE. ANT was eluted from the gel by electroelution (Electro-Eluter Model 422, Bio-Rad). The quality of the purified ANT was tested by SDS−PAGE and Coomassie blue staining, and protein concentration was measured using the Pierce protein assay reagent (Pierce Chemical Co).

Back-Titration ELISA. To analyze the reactivity of antibodies with recombinant bovine GST−ANT1, microtiter ELISA wells (Maxisorb F96 Immuno plates, Nunc) were coated with 0.5 μg of purified GST−bANT1 in carbonate buffer, pH 9.6 (Sigma), overnight at 4 °C and then blocked with 0.5% skimmed milk (Molico, Nestlé), 0.1%Tween-20 in PBS (Sigma). Antibody reactivity was detected using standard ELISA protocols. Briefly, 0.1 mL of appropriate dilutions of mouse antibodies was added to triplicate wells and incubated for 2 h at room temperature. After being washed with PBS, the wells were incubated with 0.1 mL of a 1/50000 dilution of peroxidase-conjugated goat purified IgG anti-mouse IgG (Bio-Rad) for 2 h at room temperature. Antibody reactivity was detected by the addition of peroxidase substrate [3.7 mmol/L 1,2-phenylenediamine (Merck), 0.2 μL/mL H_2O_2 30% in 0.15 mol/L citrate buffer, pH 5], and absorbance was recorded by an automated ELISA plate reader (Titertek Multiscan MKII Plus, Flow Laboratories) at 492 nm. Competition studies were performed by incubating the mouse antibodies with various GST−ANT constructs and peptides at a concentration ranging between 0.1 and 10 μg/mL in blocking solution for 1 h at room temperature in an orbital shaker. They were then analyzed by ELISA as described above, and the percentage of inhibition was calculated from the values with and without competitor. To analyze the reactivity of mouse antibodies against native membrane-bound ANT, ELISA plates were coated with broken mitochondrial membranes and incubated with appropriate dilutions of mouse antibodies pretreated or not with competitors as above. To determine the orientation of loops M2 and M3 of native ANT, back-titration ELISA was performed. ELISA plates were coated with broken mitochondrial membranes, and mouse antibodies were reacted with them. These antibodies were also pretreated with mitoplasts and SMP as competitors. In these experiments, the antibody solutions that were incubated with mitoplasts and SMP were diluted with an isotonic buffer (0.25 M sucrose, 1 mM EGTA, 10 mM Tris-HCl, pH 7.4) to avoid the rupture of mitoplasts and SMP.

Cloning and Expression of GST−ANT Fusion Proteins. The bovine ANT1 isoform was produced as a GST fusion protein as described elsewhere (*12*). Total RNA from bovine heart was reverse transcribed (RT) using the AMV reverse transcription system (Promega) with an oligo$(dT)_{15}$ primer. The resulting cDNAs were used as templates for the amplification with Taq DNA polymerase (Promega) and specific primers in a PCR system (Minicycler, MJ Research) to clone the coding sequences of the bovine ANT1 isoform, according to the published sequence (*18*). The primers were designed so that the resulting PCR products contained a *Bam*HI recognition sequence at the 5′ end and an *Eco*RI recognition site at the 3′ end for direct in-frame cloning into the pGEX-1λT vector (Pharmacia) to express ANTs in HB101 *Escherichia coli* as GST−ANT fusion proteins. The oligonucleotides used were the following: for bANT1 forw 5′-CCCGGATCCGATCAGGGCTCTGAGCTTCCTG-3′ and rev 5′-GGGGAATTCTTTTTGATCTCATCATACAA-3′. These oligonucleotides allowed the cloning of the complete coding region of ANT1 except for the first methionine and the last two C-terminal amino acids. Partial constructs (Figure 1A) were obtained by PCR using purified pGEX-ANT1 DNA as the template and the following set of oligonucleotides: Nt construct, forw 5′-GTCGGATCCGGTGATCACGCTTGGAGCTTCCTA-3′ and rev 5′-CCCGAATTCCAGCGGGTAGACAAAGCA-3′. The PCR product of 417 nt coded for amino acids 1−133 of the complete ANT1 isoform. Ct construct: forw 5′-CCCGGATCCGACTTTGCTAGGACCAGG-3′ and rev 5′-GGGGAATTCTTTTTGATCTCATCATACAA-3′. The PCR product of 503 nt coded for amino acids 133−297 of ANT1. Ct1 construct: forw 5′-CCCGGATCCGACTTTGCTAGGACCAGG-3′ and rev 5′-CCCGAATTCACCCTGGTAGACCCCCCT-3′. The PCR product of 441 nt coded for amino acids 133−276 of ANT1. Ct2 construct: forw 5′-CCCGGATCCGACTTTGCTAGGACCAGG-3′ and rev 5′-CCCGAATTCTCTACGACGAACAGTGTC-3′. The PCR product of 327 nt coded for amino acids 133−238 of ANT1. LM2 construct: forw 5′-CCCGGATCCGACTTTGCTAGGACCAGC-3′ and rev 5′-C-

CCGAATTCACCCTGGTAGAGCCCCCT-3′. The PCR product of 144 nt coded for amino acids 133−176 of ANT1 (putative loop M2). Cti construct: forw 5′-CCCGGATCCAGGGGGCTCTACCAGGGT-3′ and rev 5′-CCCGAATTCTCTACGACGAACAGTGTC-3′. The PCR product of 219 nt coded for amino acids 169−238 of ANT1 (putative region interloops M2 and M3). LM3 construct: forw 5′-CCCGGATCCGACACTGTTCGTCGTAGA-3′ and rev 5′-CCCGAATTCCCAGGCACCTTTGAAGAA-3′. The PCR product of 150 nt coded for amino acids 231−276 of ANT1 (putative loop M3). Ct3 construct: forw 5′-CCCGGATCCAGGGGGCTCTACCAGGGT-3′ and rev 5′-CCCGAATTCCCAGGCACCTTTGAAGAA-3′. The PCR product of 333 nt coded for amino acids 169−276 of ANT1. The *Bam*HI and *Eco*RI restriction sequences are underlined. The PCR products were purified and ligated to pGEX-1λT as described above. All of the constructs were verified by automated sequencing (SCT; University of Barcelona). Transformed HB101 *E. coli* cells were induced with 0.5 mmol/L IPTG for 4 h to express the fusion proteins. Fusion proteins were expressed as inclusion bodies, which were further purified by centrifugation in a sucrose density gradient as described elsewhere (*12*). GST was affinity-purified with glutathione−Sepharose (Pharmacia) from an extract of HB101 cells transformed with pGEX-1λT. GST−ANT1 fusion proteins were purified from inclusion bodies by ChromaPhor as for mitochondrial ANT.

Immunoblotting. Purified GST and bovine ANT and GST−ANT fusion proteins were separated on 12% PAGE minigels and electrotransferred to PVDF membranes (Immobilon-P, Millipore). Membranes were blocked with 5% skimmed milk and 0.1% Tween-20 in PBS, probed with mouse ascitic fluids at appropriate dilutions, and then incubated with horseradish peroxidase-conjugated purified goat IgG antimouse IgGs (Bio-Rad) diluted 1/3000. Detection was performed by enhanced chemiluminescence (ECL; Amersham). Alternatively, blots were probed with a goat anti-GST serum (Pharmacia) to ensure equal loading of fusion proteins.

Epitope Scanning. Spots epitope scanning kits were obtained from Cambridge Research Biochemicals and Genosys. All procedures, including the regeneration of the membranes for multiple uses, were carried out as described in the kit manual, with the exception of the final detection of spots. Decapeptides with eight overlapping amino acids spanning the 2/3 C-terminal amino acid sequence of ANT1 were synthesized on derivative cellulose membranes and probed with mouse antibodies at appropriate dilutions and horseradish peroxidase-conjugated affinity purified IgG antimouse IgGs (Bio-Rad) diluted 1/3000. Spots were detected by ECL (Amersham).

Peptides. Peptides corresponding to the three short sequences of the human ANT1 isoform were synthesized at the Peptide Synthesis Service (University of Barcelona) and used as competitors in the back-titration ELISA. Peptide A: 132-DFARTRLAADVGK-146. Peptide B: 137-RTRLAADVGKGAAQ-150. Peptide 1: 160-IIKIFKSDGLRGL-172.

Antibody Production against Bovine Heart ANT. Antibodies against purified bovine heart ANT were raised by inducing the production of ascitic fluid in mice basically as described in ref *19*. Purified ANT (40−60 μg) was used as antigen and administered ip in a total volume of 0.2 mL with

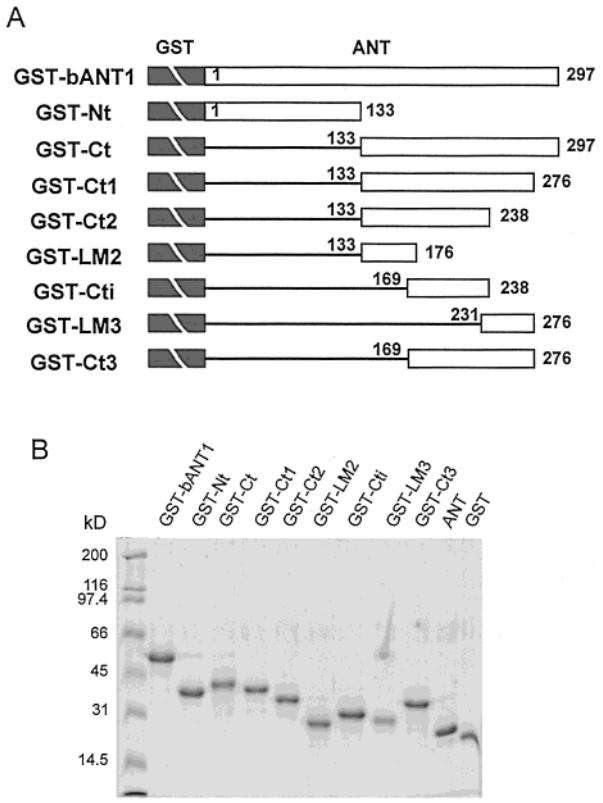

FIGURE 1: (A) Scheme of the constructs of the GST−ANT fusion protein produced. The GST moiety of the fusion proteins is represented by broken gray boxes and the ANT moiety by open boxes. The nomenclature of the fusion proteins is indicated at the left and defined in the Experimental Procedures section. The amino acids of each construct, corresponding to the bovine ANT1 sequence, are indicated. (B) A Coomassie blue stained gel of the GST−ANT fusion proteins and purified bovine heart ANT and purified GST is shown along a molecular weight marker.

complete Freund adjuvant (Sigma) in a 1:9 v/v antigen: adjuvant ratio on days 0, 14, 21, 28, 35, 42, and 49 to four male Balb/c mice. Thereafter, ascitic fluid was recovered by ip puncture with a sterilized 21-G gauge. After the extraction, ascitic fluids were incubated for 30 min at 50 °C and centrifuged at 10000*g* for 10 min at room temperature. The supernatants were stored at −20 °C until use. These four supernatants are referred to as ascitic fluids or antibodies (named Ab no. 1, Ab no. 2, Ab no. 3, and Ab no. 4) throughout the paper. This procedure was performed following the United Kingdom Coordinating Committee on Cancer Research (UKCCCR) Guidelines for the Welfare of Animals in Experimental Neoplasia (1997).

RESULTS

Characterization of Ascitic Fluids. To characterize the ascitic fluids (Ab no. 1, Ab no. 2, Ab no. 3, and Ab no. 4) obtained after the immunization of four mice with purified bovine ANT, we designed a set of partial constructs of ANT, taking advantage of the high bacterial expression of the GST−ANT fusion proteins. The partial constructs were designed to cover the putative transmembrane and hydrophilic loops of the C-terminal half of the protein. The complete and partial constructs of ANT as fusion proteins with GST are schematized in Figure 1A. A Coomassie-stained PAGE of the purified proteins, including complete

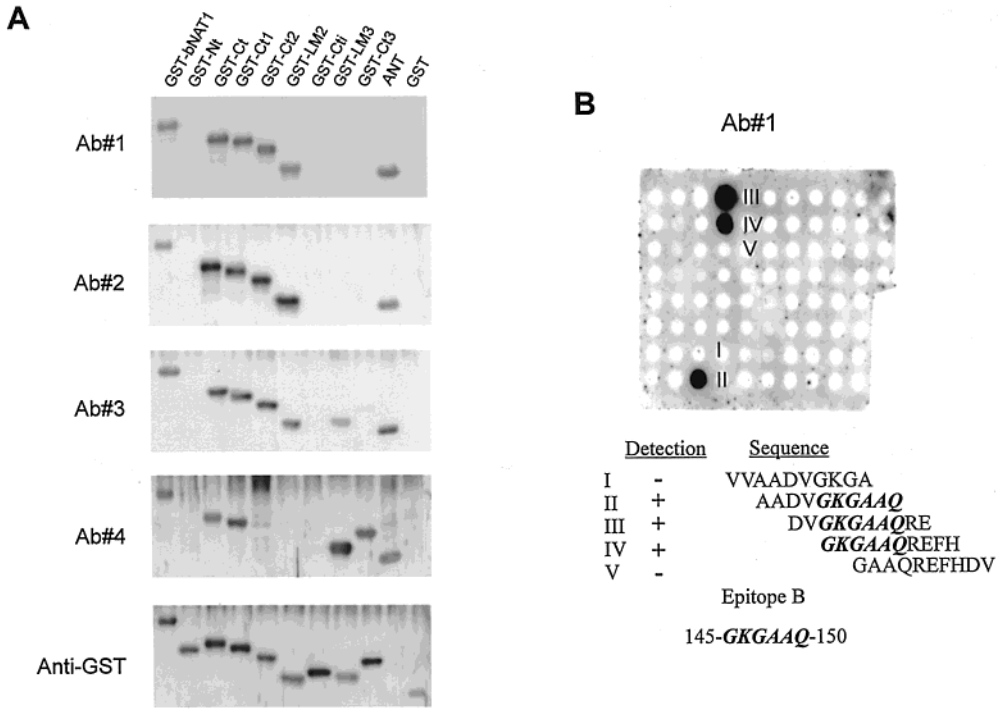

FIGURE 2: (A) Examples of immunoblots with the four murine antibodies and an antibody against GST. Dilutions of the antibodies were the following: Ab no. 1 at 1/50000, Ab no. 2 at 1/4000, Ab no. 3 at 1/15000, and Ab no. 4 at 1/30000. GST antiserum was used at a 1/200 dilution. (B) Spot analysis corresponding to Ab no. 1 and a preimmune murine serum. Spot membranes were incubated with Ab no. 1 at a dilution of 1/50000. The preimmune serum was used at a dilution of 1/1000. The analysis of epitope B is indicated. The sequence of spots I−V is indicated along with the detection (+) or lack of detection (−) with Ab no. 1. The amino acids required to react with the antibody are in cursive type and bolded.

and partial constructs of ANT as fusion proteins, and purified bovine heart ANT and GST is shown in Figure 1B. Preliminary experiments were designed to titrate the ascitic fluids obtained and thus select the optimal dilution of the antibodies. Experimental antibodies against bovine ANT were characterized by Western blot with the purified ANT proteins (Figure 2A). None of the antibodies reacted with the N-terminal half of the protein (construct GST−Nt), ruling out the presence of major immunogenic regions in the first 133 amino acids of ANT. Ab no. 1 and Ab no. 2 showed similar behavior in these analyses (Figure 2B). They reacted with bovine isoform ANT1, fused or not to GST. Ab no. 1 and Ab no. 2 reacted with the C-terminal half of the protein (construct GST−Ct). This reaction was not dependent on the presence of the last 21 amino acids of the protein, GST−Ct1, or the last 59 amino acids, GST−Ct2. Finally, they reacted with the construct GST−LM2, which comprises the putative loop M2, but not with constructs lacking amino acids 133−176. Therefore, both antibodies recognized loop M2 as the main immunogenic region of ANT. Ascitic fluid Ab no. 3 (Figure 2A) showed a similar result, but in addition to loop M2, it also recognized a region within loop M3, since it reacted with the GST−LM3 construct. This antibody did not react with construct GST−Ct3, which contains the region of loop M3 plus the last intramembrane segment. Differences in the spatial structure of these constructs may account for this otherwise puzzling result. Ab no. 4 reacted preferentially with the constructs GST−LM3 and GST−Ct3 but not with the construct GST−LM2, demonstrating that the main recognized region is located in loop M3 (Figure 2A). Therefore, loops M2 and M3 had the most immunogenic regions of ANT. Figure 2A also shows the same membrane with an anti-GST antibody, confirming the equal loading of proteins in the gel.

Table 1: Antigenic Determinants on the ANT1 Isoform Determined with Spot Membranes

antibody	epitope	sequence	location
Ab no. 1	B	145-GKGAAQ-150	loop M2
Ab no. 2	A	133-LDFARTRL-140	loop M2
	B	145-GKGAAQ-150	loop M2
Ab no. 3	B	145-GKGAAQ-150	loop M2
	C	230-FDTVRRRM-237	loop M3
Ab no. 4	D	244-KGADIMYT-251	loop M3

In an attempt to identify the amino acids recognized by the various antibodies, we performed an epitope scanning analysis with overlapping decapeptides covering the human ANT1 sequence, synthesized on solid support. An example of the results obtained with Ab no. 1 and the definition of its epitope are shown in Figure 2B. Preimmune sera were unreactive with peptides (results not shown). The results obtained with the four murine antibodies are presented in Table 1. We defined four antigenic determinants named epitopes A−D. Ab no. 1 recognized a unique epitope, epitope B, 145-GKGAAQ-150, localized in loop M2. Ab no. 2 defined two regions very close in sequence but clearly distinct, epitope A, 133-LDFARTRL-140, and the above-defined epitope B, both located in loop M2. Ab no. 3 detected two epitopes, epitope B in loop M2 and epitope C, 230-FDTVRRRM-237, located in loop M3. Finally, Ab no. 4 reacted with only one epitope, epitope D, 244-KGADIMYT-251, located in loop M3. Thus, the sequence of epitope B seemed to be immunodominant, since it reacted with three out of four ascitic fluids. We would like to highlight the

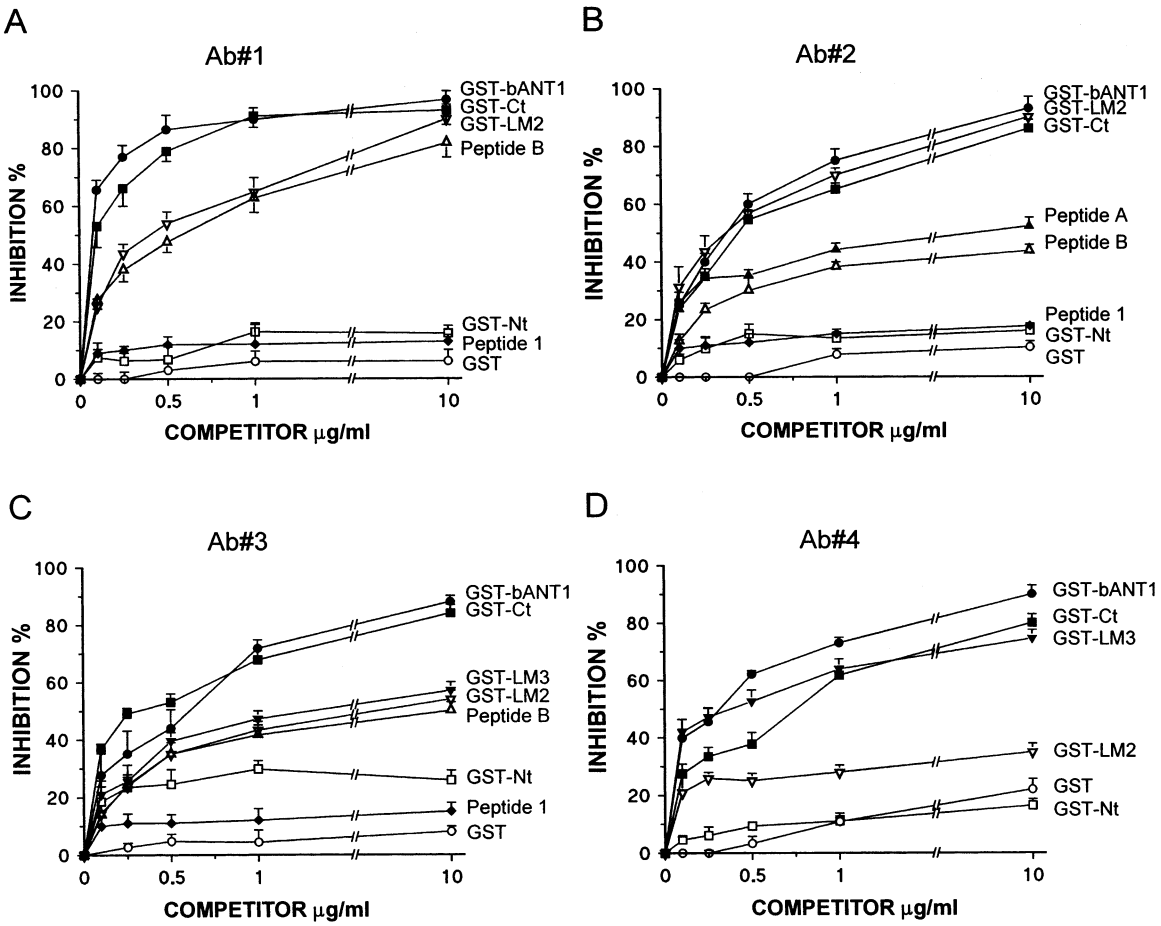

FIGURE 3: Back-titration ELISA with GST−ANT1 coated microplates of the murine antibodies. Antibodies were preincubated with various concentrations of complete GST−ANT1 fusion protein, with partial constructs, with purified GST, or with peptides as indicated. The results (mean ± SEM of three independent experiments) are expressed as the percent of the inhibition with respect to the value of the absorbance obtained without preincubation of the antibodies.

correlation between the Western blot and the spot analysis results, stressing the very short epitope spreading of the antibodies obtained.

Back-Titration ELISA with Recombinant GST−bANT1 Fusion Protein. To study the ascitic fluids against ANT and to examine the relative contribution of the epitopes in the detection of the complete ANT, we undertook a back-titration ELISA. The ELISA plates were coated with recombinant GST−bANT1 fusion protein, and the reaction of the antibodies competed with several GST−ANT fusion proteins and peptides (Figure 3). The detection of recombinant GST−ANT1 fusion protein by the four antibodies did not compete with GST, pointing to the specificity of the reaction, nor with GST−Nt, demonstrating the absence of significant epitopes in the N-terminal half of the protein. In contrast, GST−Ct competed to the same extent as complete ANT1, indicating that this region contains the major epitopes responsible for the detection of the complete ANT (Figure 3). All of these results agree with immunoblotting data (Figure 2A). The reaction of Ab no. 1 with ANT1 competed with GST−LM2 and to the same extent with peptide B, which contains the sequence of epitope B as determined by the Spot analysis (Table 1). Another peptide corresponding to sequence 160−172 of ANT1 (peptide 1), which does not carry any detected epitope, was thus without effect (Figure 3A). These results clearly demonstrate that epitope B is the main antigenic determinant involved in the reaction of Ab no. 1 with ANT. Like Ab no. 1, Ab no. 2 reacted with complete ANT through epitopes in loop M2 (Figure 3B), two in fact as revealed by the Spot analysis. The inhibition of the reaction by peptide B and peptide A was similar (Figure 3B), indicating an equal contribution of both epitopes to the reaction of Ab no. 2 with the complete ANT. Peptide 1 was also without effect. The reaction of Ab no. 3 with recombinant GST−bANT1 fusion protein was partially competed by the GST−Nt construct, suggesting the presence of some minor epitope(s) in the N-terminal half of ANT that had not been detected by Western blot (Figure 3C). Ab no. 3 reacted with two epitopes, one residing in loop M2 and the another in loop M3 (Figure 2A and Table 1). The two loops inhibited the detection of the full ANT1 in the back-titration ELISA to a similar extent and, hence, contributed equally to the overall detection of ANT. Moreover, Ab no. 3 reacted with loop M2 through the sequence corresponding to epitope B (Figure 3C). Ab no. 4 was shown to react mainly with an epitope in loop M3. Back-titration ELISA (Figure 3D) shows that, in agreement with the immunoblot analysis, the construct GST−LM3 competes to a higher extent than the construct GST−LM2. Hence, the epitope in loop LM3 accounted for the major detection of ANT with Ab no. 4, although minor epitopes in loop M2 are now apparent.

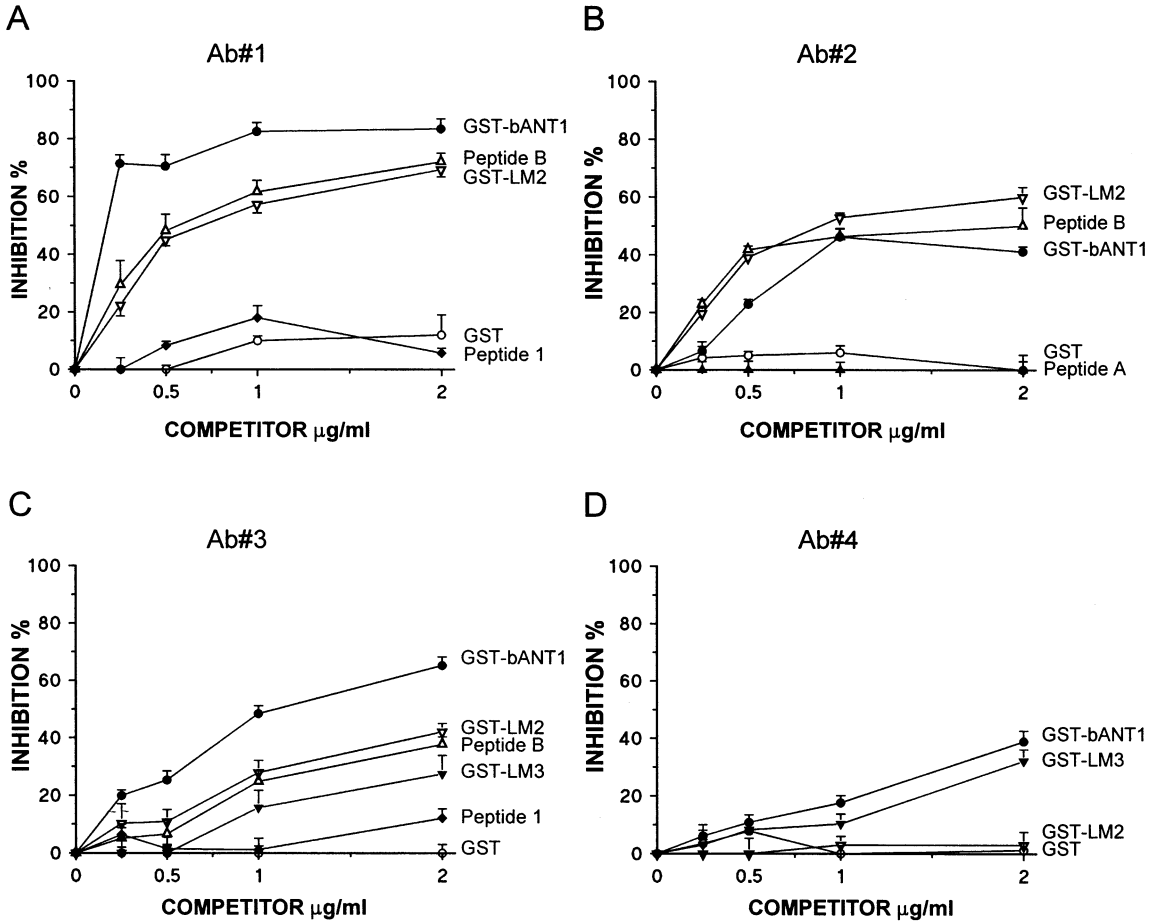

FIGURE 4: Back-titration ELISA with native ANT. Microplates were coated with mitochondrial membrane fragments and incubated with the murine antibodies preincubated with various concentrations of complete GST−ANT1 fusion protein, with partial constructs, with purified GST, or with the peptides as indicated. The results (mean ± SEM of three independent experiments) are expressed as the percent of the inhibition with respect to the value of the absorbance obtained at 492 nm without preincubation of the antibodies. The antibodies were used at the following dilutions: Ab no. 1 at 1/50000, Ab no. 2 at 1/2000, Ab no. 3 at 1/15000, and Ab no. 4 at 1/30000.

Back-Titration ELISA with Native ANT. Once the binding properties of the ascitic fluids had been characterized, we examined the native conformation of ANT in the inner mitochondrial membrane. A model of the topography of ANT that summarizes the results is depicted in Figure 7. In the next experiment, ELISA plates were coated with fragments of the inner mitochondrial membrane from bovine heart, and the reaction with the ascitic fluids was competed with several constructs and peptides (Figure 4). The reaction of Ab no. 1 with broken inner mitochondrial membranes competed effectively with recombinant GST−bANT1 (Figure 4A). Similar inhibition was observed with the construct GST−LM2 and with peptide B (amino acids 137−150), indicating that the major epitope (amino acids 145−150) involved in this reaction was fully accessible to the antibodies and was thus located outside the membrane in the native structure of ANT. The lack of inhibition by both GST and peptide 1 confirms the specificity of the inhibition obtained with the other competitors. Ab no. 2 reacted with ANT through two very close amino acid sequences located in loop M2 (amino acids 133−140 and 145−150). In back-titration ELISA with broken inner membranes, construct GST−LM2 and peptide B were effective inhibitors of the reaction with GST−bANT1, thus confirming the external location of this sequence in the native ANT (Figure 4B). In contrast, peptide A, carrying epitope A, did not inhibit the reaction. Hence, it can be assumed that region 133−140 is embedded either in the membrane or in the native protein, folded in such a way that it is no longer accessible to the antibodies. Ab no. 3 interacted with ANT mainly through two short sequences located in loops M2 and M3. The reactivity of Ab no. 3 with the native ANT inserted in the membrane was effectively inhibited by GST−bANT1, like that of Ab no. 1 and Ab no. 2 (Figure 4C). The constructs GST−LM2 and GST−LM3 similarly inhibited the reaction with native ANT, each achieving one-half of the inhibition produced by GST−bANT1. This strongly suggests that both epitopes, i.e., amino acids 145−150 and 230−237, contribute equally to the overall recognition of the native ANT and are accessible to the antibodies, and thus lie outside the membrane. Finally, the results obtained with Ab no. 4 differed (Figure 4D). This ascitic fluid mainly recognized an epitope in loop M3, amino acids 244−251. This antibody was scarcely reactive with the native ANT (results not shown). Moreover, we observed a very poor competition with both GST−bANT1 and construct GST−LM3 in the back-titration ELISA with native ANT (Figure 4D), suggesting that sequence 244−251 was not fully accessible to the antibodies, although it belongs to loop M3.

Studies on the Orientation of Loops M2 and M3. After showing that amino acid sequence 145−150 is outside native ANT, we studied the orientation of loop M2 (matrix or

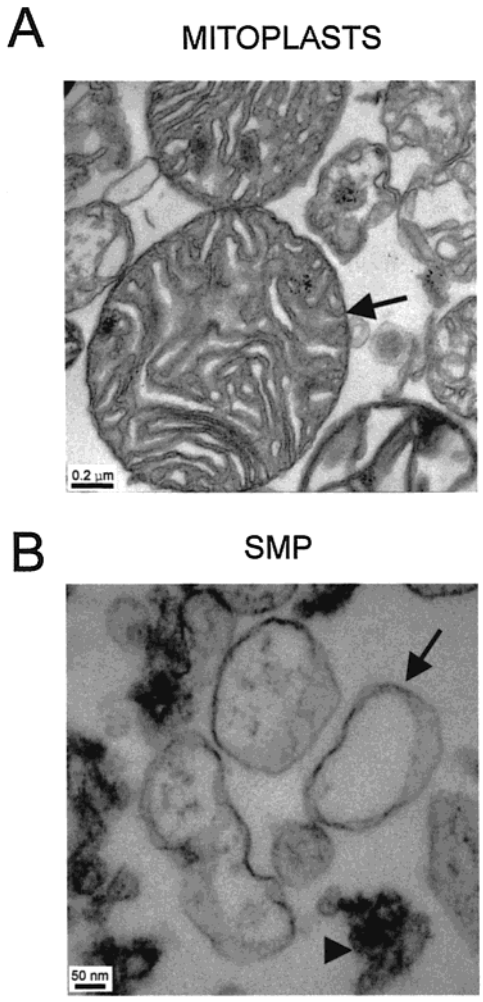

FIGURE 5: Mitoplasts and SMP ultrastructure. Bovine heart mitochondria were subjected to freeze−thaw cycles to obtain mitoplasts. SMP were obtained by sonication of the mitoplasts in the appropriate buffer as described under the Experimental Procedures section. (A) Microphotograph of mitoplasts (arrow) showing the lack of outer mitochondrial membrane and the presence of the typical mitochondrial cristae. (B) Microphotograph of SMP showing their vesicular morphology (arrow). Some proteinaceous corpuscles can be observed (arrowhead). Note the different scale of both microphotographs.

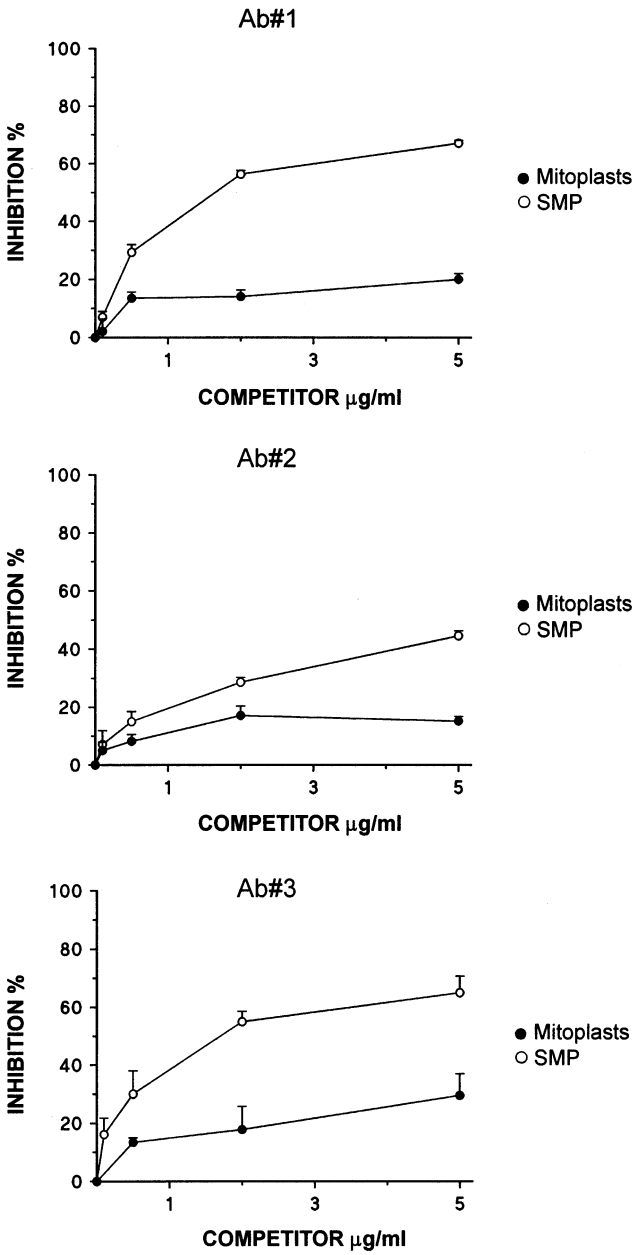

FIGURE 6: Determination of the orientation of loops M2 and M3 by back-titration ELISA. Microplates were coated with mitochondrial membrane fragments and incubated with Ab no. 1, Ab no. 2, and Ab no. 3. The reaction was competed by preincubation of the antibodies with various concentrations of mitoplasts and SMP. Results (mean ± SEM of three independent experiments) are expressed as the percent of inhibition of the absorbance at 492 nm without the competitor. The antibodies were used at the following dilutions: Ab no. 1 at 1/50000, Ab no. 2 at 1/2000, Ab no. 3 at 1/15000, and Ab no. 4 at 1/30000.

cytosol) to support the conformation model of ANT as a six or five transmembrane protein. In this case, the ELISA plates were coated with broken inner membranes, and the reaction was competed with mitoplasts (mitochondria without external membrane) and SMP (submitochondrial particles with an inside-out orientation of the inner mitochondrial membrane) (see the Experimental Procedures section). A microphotograph of mitoplasts and SMP shows the absence of external membrane in the mitoplast fraction (Figure 5A) and the vesicular aspect of SMP (Figure 5B). Note the different size of the samples: SMP were much smaller than mitoplasts. The integrity of the inner mitochondrial membrane of the mitoplast preparation was confirmed by its inability to oxidize NADH added externally, in comparison with broken membranes and SMP, which oxidized NADH at a high rate (data not shown). The results obtained by competing the reactivity of ascitic fluids with native ANT with these preparations of mitochondrial membranes are shown in Figure 6. Ab no. 1, Ab no. 2, and Ab no. 3 showed similar behavior. Competition with SMP was always higher than with mitoplasts, indicating the inaccessibility of epitope B to antibodies from the cytoplasmic side and its accessibility from the matrix side, and rules out a significant contamination of mitoplasts with broken inner membranes. Ab no. 4 was not tested owing to its inability to react with native ANT, as described above. The inside-out membrane orientation of SMP was verified by using a monoclonal antibody against subunit IV of cytochrome oxidase, which is known to react with an epitope located in the intermembrane space of mitochondria (*17*). The reactivity of this antibody to frag-

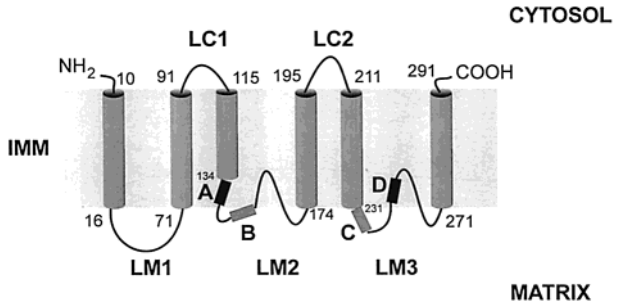

FIGURE 7: Schematic representation of the topography of ANT in the inner mitochondrial membrane based on the model by Majima et al. (*11*). The location of the antigenic determinants (regions A, B, C, and D) on ANT described with the murine antibodies is indicated. The regions accessible to the antibodies are represented by light gray boxes. Those regions that are inaccessible to the antibodies are represented by dark gray boxes. This representation intends to explain the accessibility of regions B (145−150) and C (230−237) and the inaccessibility of regions A (133−140) and D (244−251) in light of actual knowledge of the topography of ANT and the results of this study. The matrix orientation of loops M2 and M3 is also indicated.

ments of mitochondrial membranes competed with mitoplasts but did not compete with SMP (data not shown). Thus, the results demonstrate that loop M2, which contains region 145−150 (epitope B), has a matrix orientation. Furthermore, since Ab no. 3 also reacted with epitope C (amino acids 230−237), and its reaction with native ANT is more effectively competed with SMP than with mitoplasts, we can extend this conclusion to loop M3 (see Figure 7).

DISCUSSION

We raised antibodies against purified bovine heart ANT by producing ascitic fluid in mice. This methodology resulted in the generation of antibodies against ANT with a marked antigenic determinant spreading restriction. Thus, the four ascitic fluids interacted with ANT through only one or two short amino acid sequences. Antibodies reacted with linear short peptides rather than with conformational epitopes, which is most likely due to the denatured state of the purified ANT used by immunization. Although computer prediction of the antigenic determinants of ANT showed that they are spread over the whole sequence of ANT (*13*), we found no evidence of the presence of antigenic determinants in the first 133 amino acids of ANT in Western blot or ELISA analysis, suggesting that this region is rather poorly immunogenic. In contrast, the C-terminal half of the protein contains the highest immunogenicity, especially the amino acid regions that form the putative hydrophilic loops M2 and M3. These results are consistent with those obtained in the characterization of the autoantibodies against ANT in IDCM patients, which located the main epitopes in loops M2 and M3 (*12*). This suggests that the autoimmune response in IDCM reflects the higher immunogenicity of these regions rather than a specific response of the disease. On the other hand, the well-characterized antigenic determinants allowed us to use the murine antibodies to study the membrane-bound topography of ANT. First, we aimed to determine the accessibility of these regions to the antibodies in the native ANT (the results are summarized in Figure 7). It has been proposed that the hydrophilic loops M2 and M3 contained amphipathic segments, amino acids 140−151 and 153−167 in M2 and amino acids 237−249 and 253−276 in M3 that crossed the membrane as β sheets or short α helices (*3*, *8*). Majima et al. (*7*), by analyzing the reactivity of cysteines to SH reagents, *N*-ethylmaleimide (NEM) and eosin 5-maleimide (EMA), concluded that Cys-159, in the middle of loop M2, and Cys-256, in the middle of loop M3, were not exposed to the membrane surface and that these loops may intrude into the membrane. Our results can be discussed in the light of these proposals. We show that region 145−150 in loop M2 and region 230−237 in loop M3 are fully accessible to the antibodies when ANT is in the native state, indicating that these regions are not embedded in the membrane. They are probably adjacent to the segments really intruded into the membrane. Our results also demonstrate that region 133−140 is inaccessible to the antibodies. According to the hydropathy plots of ANT, this sequence belongs to the hydrophilic loop M2 (*20*). The lack of reactivity with the antibodies suggests that it is probably too close to the membrane, at the end of a transmembrane segment, in agreement with the most accepted model of ANT topography (*1*, *7*; Figure 7). Finally, region 244−251 was reactive to antibodies in denatured protein but largely nonreactive in native protein. This region is very close to the Cys-256 mentioned above, which supports the hypothesis that loop M3 has a segment that intrudes into the membrane, making this region inaccessible to the antibodies. An alternative explanation to the lack of reactivity of regions 133−140 and 244−251 is that these regions are hidden by the folding of loops M2 and M3 in the native protein. In this sense, it has been reported that antibodies can be very sensitive to the conformation of ANT (*21*). Our results cannot discern between the two alternatives. Nevertheless, the partial membranous characteristic of loops M2 and M3 is consistent with several proposed models of the insertion of ANT into the membrane (refs *3*, *7*, and *8*, among others). Accordingly, we present (Figure 7) a model of the topography of ANT in the mitochondrial membrane, based on that of ref *7*, according to ref *1*, in which the accessibility of regions 145−150 and 230−237 and the inaccessibility of regions 133−140 and 244−251 to the antibodies are shown.

The topography of the membrane-bound ANT is controversial. Using hydropathy plots, a model with six transmembrane segments was proposed (*20*). This model is based on the triplicate structure of ANT deduced from the analysis of the amino acid sequence. Each triplicate consisting of two transmembrane segments joined by a large hydrophilic segment and these repeats are linked to each other by short hydrophilic segments. By analogy to other members of the solute mitochondrial transporter family such as uncoupling protein-1 (UCP-1) (*22*, *23*) and phosphate carrier (*24*), it was supposed that the N-terminal and C-terminal ends of ANT face the cytosol and the three hydrophilic loops face the matrix and so they were named loops M1, M2, and M3. Using antibodies against a peptide of the N-terminal end of ANT, it was shown that the N-terminal end had a cytosolic orientation (*2*), but the results obtained with antibodies against the C-terminal end were inconclusive regarding the orientation of this end (*2*). Moreover, a number of experimental results on the orientation of hydrophilic loops were interpreted in opposing ways. Thus, the labeling of membrane-bound ANT with 2-azido-ADP and azidoatractyloside indicated that the fragments spanning amino acids 153−200 and

250−281 face the cytosol (*4*, *5*), whereas enzymatic proteolysis (*3*) and labeling with SH reagents EMA and NEM (*6*, *7*) indicated that loops M2 and M3 face the matrix. In addition, Dalbon et al. (*4*) and Marty et al. (*3*) proposed a model of ANT conformation consisting of five transmembrane segments, since the putative second transmembrane segment is poorly hydrophobic. In this model of five transmembrane segments, the N-terminal and C-terminal ends are oriented toward opposite sides of the membrane, N-terminal end facing the cytosol and the C-terminal end facing the matrix. Accordingly, loops M2 and M3 are oriented toward the cytosol, in contrast to the six transmembrane segment model. We studied the orientation of loops M2 and M3 using mitoplasts, devoid of outer membrane, and SMP, with inside-out orientated membranes, in a back-titration ELISA with fragments of inner mitochondrial membrane-coated plates. We took advantage of the precisely defined antigenic determinants that reacted with the antibodies we raised on ANT. We demonstrated that the reaction of region 145−150 of loop M2 and region 230−237 of loop M3 with the antibodies competed with SMP, but to a much lesser extent with mitoplasts, indicating that these regions face the matrix side of the membrane. Therefore, our data support a matrix orientation of loops M2 and M3 and so the six transmembrane segment model of ANT conformation in the inner mitochondrial membrane as depicted in Figure 7.

In summary, we raised murine antibodies against ANT with a short spreading of antigenic determinants. Results revealed the high immunogenicity of loops M2 and M3, in sharp contrast with loop M1. Furthermore, we used these antibodies to study the topography of native ANT. We found that region 145−150, in loop M2, and region 230−237, in loop M3, are fully accessible to the antibodies, which indicates that they lie outside the membrane. In contrast, the inaccessibility of regions 133−140 and 244−251 supports their insertion into the inner mitochondrial membrane. Finally, we demonstrated that loops M2 and M3 face the matrix, supporting the six transmembrane domain model of ANT conformation.

REFERENCES

1. Klingenberg, M. (1989) *Arch. Biochem. Biophys. 270*, 1−14.
2. Brandolin, G., Boulay, F., Dalbon, P., and Vignais, P. V. (1989) *Biochemistry 28*, 1093−1100.
3. Marty, I., Brandolin, G., Gagnon, J., Brasseur, R., and Vignais, P. (1992) *Biochemistry 31*, 4058−4065.
4. Dalbon, P., Brandolin, G., Boulay, F., Hoppe, J., and Vignais, P. V. (1988) *Biochemistry 27*, 5141−5149.
5. Boulay, F., Lauquin, G. J. M., Tsugita, A., and Vignais, P. V. (1983) *Biochemistry 22*, 477−484.
6. Boulay, F., and Vignais, P. V. (1984) *Biochemistry 23*, 4807−4812.
7. Majima, E., Koike, H., Hong, Y. M., Shinohara, Y., and Terada, H. (1993) *J. Biol. Chem. 268*, 22181−22187.
8. Bogner, W., Aquila, H., and Klingenberg, M. (1986) *Eur. J. Biochem. 161*, 611−620.
9. Hatanaka, T., Hashimoto, M., Majima, E., Shinohara, Y., and Terada, H. (1999) *Biochem. Biophys. Res. Commun. 262*, 726−730.
10. Trézéguet, V., Le Saux, A., David, C., Goudert, C., Fiore, C., Dianoux, A. C., Brandolin, G., and Lauquin, G. J. M.. (2000) *Biochim. Biophys. Acta 1457*, 81−93.
11. Schultheiss, H. P., and Bolte, H. D. (1985) *J. Mol. Cell. Cardiol. 17*, 603−617.
12. Manchado, C., Orus, J., Villarroya, F., Roig, E., Heras, M., Giralt, M., Iglesias, R., Sanz, G., Mampel, T., and Viñas, O. (2002) *J. Mol. Cell. Cardiol. 34*, 571−582.
13. Schwimmbeck, P. L., Schwimmbeck, N. K., Schultheiss, H. P., and Strauer, B. E. (1993) *Clin. Immunol. Immunopathol. 68*, 135−140.
14. Smith, A. L. (1967) *Methods Enzymol. 10*, 81−86.
15. Lauquin, G. J. M., Villiers, C., Michejda, J. W., Hryniewiecka, L. V., and Vignais, P. V. (1977) *Biochim. Biophys. Acta 460*, 331−345.
16. Fioravanti, C. F., McKelvey, J. R., and Reisig, J. M. (1992) *J. Parasitol. 78*, 774−778.
17. Tsukihara, T., Aoyama, H., Yamashita, E., Tomizaki, T., Yamaguchi, H., Shinzawa-Itoh, K., Nahashima, R., Yaono, R., and Yoshikawa, S. (1996) *Science 272*, 1136−1144.
18. Powell, S. J., Medd, S. M., Runswick, M. J., and Walker, J. E. (1989) *Biochemistry 28*, 866−873.
19. Harlow, E., and Lane, D. (1988) in *Antibodies, a laboratory manual*, Cold Spring Harbor Laboratory, Cold Spring Harbor, NY.
20. Saraste, M., and Walker, J. E. (1982) *FEBS Lett. 144*, 250−254.
21. Buchanan, B. B., Eiermann, W., Riccio, P., Aquila, H., and Klingenberg, M. (1976) *Proc. Natl. Acad. Sci. U.S.A. 73*, 2280−2284.
22. Eckerskorn, C., and Klingenberg, M. (1987) *FEBS Lett. 226*, 166−170.
23. Miroux, B., Frossard, V., Raimbault, S., Ricquier, D., and Bouillaud, F. (1993) *EMBO J. 12*, 3739−3745.
24. Capobianco, L., Brandolin, G., and Palmieri, F. (1991) *Biochemistry 30*, 4963−4969.

BI020528B